

# Search for an Admixture of a 17 keV Neutrino in the $\beta$ Decay of $^{35}\text{S}$

S. Müller<sup>1</sup>, Chen Shiping<sup>3</sup>, H. Daniel<sup>1</sup>, O. Dragoun<sup>2</sup>, N. Dragounová<sup>2</sup>, H. Hagn<sup>1</sup>, E. Hecht<sup>1</sup>, K.-H. Hiddemann<sup>1</sup>, and A. Špalek<sup>2</sup>

<sup>1</sup> Physik-Department E18, Technische Universität München, James-Frank-Straße, D-85747 Garching bei München, Germany

<sup>2</sup> Nuclear Physics Institute, Acad. Sci. Czech Rep., CZ-25068 Řež near Prague, Czech Republic

<sup>3</sup> China Institute of Atomic Energy, P.O. Box 275 (10), Beijing 102413, China

Z. Naturforsch. **49a**, 874–884 (1994); received June 27, 1994

The  $\beta$  spectrum of a mass-separated thin  $^{35}\text{S}$  source has been measured with a small-volume Si photodiode. The energy-dependent response function of the total experimental set-up was calculated by the Monte Carlo method without any adjustable parameter. For an admixture of the hypothetical 17 keV neutrino, an upper limit of 0.59% (95% CL) was determined. Neglecting electron scattering on the spectrometer diaphragm was shown to generate a false 17 keV neutrino admixture of 0.3%.

**Key words:** Neutrino mass;  $\beta$  decay;  $\beta$  spectroscopy; Electron scattering; Electron energy loss.

## 1. Introduction

Accurate measurements of the electron or positron spectra emitted by nuclei undergoing  $\beta$  decay offer a possibility to search for massive neutrinos. A great advantage of the method is, for the case of allowed  $\beta$  transitions, that it is free of nuclear-model predictions. Moreover, the method does not require any absolute measurement of intensities. In this way, the rest mass of the electron antineutrino was recently found to be  $m_{\nu\text{L}} \leq 7.2 \text{ eV}/c^2$  at 95% CL [1].

Since 1980, the  $\beta$  spectra have also been examined for an admixture of heavier neutrinos that might be emitted in the weak-interaction process together with the customary light neutrino. There is no hint from theory about the mass of such a hypothetical particle, and  $\beta$  spectroscopy represents only part of the overall effort to find massive neutrinos in nature (see e.g. reviews of Boehm and Vogel [2] and Mößbauer [3]).

The heavy neutrino of rest mass  $m_{\nu\text{H}}$  would reveal its existence via a non-regularity (a “kink”) in the continuous  $\beta$  spectrum as well as in the Kurie plot at energy  $E_{\text{max}} - m_{\nu\text{H}} c^2$ , where  $E_{\text{max}}$  is the maximum electron energy and  $c$  the velocity of light. In addition, there would be a certain surplus of  $\beta$  particles below the kink; its magnitude would be a measure of the heavy-neutrino admixture  $|U_{\text{eH}}|^2$ .

Numerous systematic searches were carried out in the energy spectra of various  $\beta$  emitters, and a wide region,  $0.1 \text{ keV} \leq m_{\nu\text{H}} c^2 \leq 2.8 \text{ MeV}$ , was examined. In most cases, no admixture of heavy neutrinos was reported and, for  $m_{\nu\text{H}} \geq 1 \text{ keV}/c^2$ , upper limits for  $|U_{\text{eH}}|^2$  between 0.03 and 0.002 were determined.

The exception refers to the case of the 17 keV neutrino, claimed by Simpson [4] to show up in the  $\beta$  spectrum of  $^3\text{H}$  taken with a semiconductor spectrometer. The Simpson statement initiated an activity of both experimenters and theoreticians that culminated around 1991, when additional positive reports on the 17 keV neutrino appeared. In particular, these were the  $^{35}\text{S}$  measurement of Hime and Jelley [5] yielding  $|U_{\text{eH}}|^2 = (0.84 \pm 0.06 \pm 0.05)\%$  and the  $^{14}\text{C}$  experiment by Sur et al. [6] with  $|U_{\text{eH}}|^2 = (1.40 \pm 0.45 \pm 0.14)\%$ , both taken with semiconductor spectrometers. Experiments covering various nuclei are listed in Table 1 [4–26]. Theoreticians published more than ninety papers examining various consequences of such a heavy neutrino.

In the experiment described below, we used a semiconductor spectrometer because the 17 keV neutrino was reported to have been observed in many semiconductor-spectrometer experiments but never in measurements with magnetic spectrometers. The former suffered from large and not well understood electron backscattering, most of the latter from the necessity of not explained purely phenomenological “shape correction factors” to meet the measured shape of the  $\beta$  spectrum. In both cases, the results of the spectrum

Reprint requests to S. Müller.

0932-0784 / 94 / 0900-0874 \$ 06.00 © – Verlag der Zeitschrift für Naturforschung, D-72027 Tübingen



Dieses Werk wurde im Jahr 2013 vom Verlag Zeitschrift für Naturforschung in Zusammenarbeit mit der Max-Planck-Gesellschaft zur Förderung der Wissenschaften e.V. digitalisiert und unter folgender Lizenz veröffentlicht: Creative Commons Namensnennung-Keine Bearbeitung 3.0 Deutschland Lizenz.

Zum 01.01.2015 ist eine Anpassung der Lizenzbedingungen (Entfall der Creative Commons Lizenzbedingung „Keine Bearbeitung“) beabsichtigt, um eine Nachnutzung auch im Rahmen zukünftiger wissenschaftlicher Nutzungsformen zu ermöglichen.

This work has been digitalized and published in 2013 by Verlag Zeitschrift für Naturforschung in cooperation with the Max Planck Society for the Advancement of Science under a Creative Commons Attribution-NoDerivs 3.0 Germany License.

On 01.01.2015 it is planned to change the License Conditions (the removal of the Creative Commons License condition “no derivative works”). This is to allow reuse in the area of future scientific usage.

Table 1. Various experiments investigating  $\beta^-$  emitters to look for an admixture of a 17 keV neutrino.

Nucleus	$ U_{eH} ^2$ in % (CL in %)	Reference
Semiconductor spectrometers		
$^3\text{H}$	$\sim 3$	[4]
reanalysis	$1.1 \pm 0.3$	[7]
$^{35}\text{S}$	$< 0.3$ (90)	[8]
$^{35}\text{S}$	$< 0.6$ (90)	[9]
$^3\text{H}$	$0.6 - 1.6$	[7]
$^{35}\text{S}$	$0.73 \pm 0.09 \pm 0.06$	[10]
$^{14}\text{C}$	$1.40 \pm 0.45 \pm 0.14$	[6]
$^{63}\text{Ni}$	$0.99 \pm 0.12 \pm 0.18$	[11]
reanalysis	$< 0.53$ (90)	[12]
$^{35}\text{S}$	$0.84 \pm 0.06 \pm 0.05$	[5]
reanalysis	$< 0.35$ (90)	[12]
$^{35}\text{S}$	$< 0.19$ (90)	[13]
$^{63}\text{Ni}$	$< 0.15$ (90)	[14]
$^{35}\text{S}$	$-0.04 \pm 0.08 \pm 0.08$	[15]
Magnetic spectrometers		
$^{35}\text{S}$	$< 0.4$ (99)	[16]
$^{35}\text{S}$	$< 0.17$ (90)	[17]
$^{35}\text{S}$	$< 0.25$ (90)	[18]
$^{63}\text{Ni}$	$< 0.3$ (90)	[19]
$^{35}\text{S}$	$< 0.2$ (90)	[20]
$^{177}\text{Lu}$	$< 1.2$ (95)	[21]
$^{63}\text{Ni}$	$< 0.073$ (95)	[22, 23]
$^{35}\text{S}$	$0.01 \pm 0.15$	[24]
Proportional counters		
$^3\text{H}$	$< 0.4$ (99)	[25]
$^3\text{H}$	$< 0.24$ (99)	[26]

analysis were highly sensitive to the shape of the spectrometer response function. This shape was derived mostly from conversion-electron lines of radioactive sources prepared under similar conditions as the  $\beta$  sources.

Later on, the effect of electron backscattering on the spectrometer slits was recognized by the respective authors; the reanalysis of the previous positive result [5] then yielded no 17 keV neutrino with  $|U_{eH}|^2 < 0.35\%$  [12]. The latest investigators [13, 15, 22] did not find any 17 keV neutrino signature in their spectra. Ohshima *et al.* [22] derived the lowest upper limit for its admixture,  $|U_{eH}|^2 < 7.3 \times 10^{-4}$  at 95% CL; unfortunately their result, as many others, is weakened by the use of a thick source backing and hence the need to introduce a “shape correction factor”.

In this work, we investigated the  $\beta$  spectrum of  $^{35}\text{S}$  with an endpoint energy of 167 keV and a half life of 88 d. Using mass separation techniques at low energy  $^{35}\text{S}$  ions, we were able to prepare a high quality source that simultaneously fulfills all three basic requirements for reliable spectrometry: (1) small average thickness of the radioactive layer, (2) absence of local

inhomogeneities which would lead to increased energy losses in some parts of the source, and (3) thin source backing. Nevertheless, we calculated properly the effect of electron scattering on the  $\beta$  spectrum shape for our source. It is for the first time that a source of such a quality was used in an experiment employing a semiconductor spectrometer (note that only from semiconductor experiments positive results were reported). The measurements were carried out with a Si photodiode that had been tested in a magnetic  $\beta$  spectrometer. The analysis was based on the energy-dependent response function calculated by the Monte Carlo method without any adjustable parameter; the result was found to agree with the experiment. We studied systematically various disturbing effects, in particular the electron backscattering on and out of the detector, which caused problems in at least some of the previous experiments. As we were interested in an experiment as “clean” as possible we had to use low counting rates in order to avoid electronic troubles, in particular not to depend on pile-up corrections or suppression techniques. Hence our statistical precision cannot compete with the experiments with the best statistics.

## 2. Experiment

### 2.1. Radioactive Source

The source was prepared with an isotope separator equipped with a beam retardation system [27]. The charge material used was 5 mCi of  $^{35}\text{S}$  in the form of  $\text{SO}_2$  with no carrier added.  $^{35}\text{S}^+$  ions of 10 keV were implanted into a thin foil consisting of  $11 \mu\text{g}/\text{cm}^2$  copper on  $23 \mu\text{g}/\text{cm}^2$  carbon. The Cu layer was thick enough to stop 90% of the implanted ions, while the remaining 10% reached the carbon (see Figure 1). The ions were implanted in a strip of  $24 \text{ mm} \times 1 \text{ mm}$ ; the rather elongated shape was dictated by the isotope separator. The source activity was about  $0.1 \mu\text{Ci}$ . An additional source on a thick aluminum backing was prepared in order to check the homogeneity of the sources produced by our method. Autoradiographic pictures of this source showed no variation of the activity over the area exposed.

From the measured spectra, the activity was found to decay with a half life of  $88.7 \pm 1.3 \text{ d}$ , in agreement with the  $^{35}\text{S}$  half life of  $87.51 \pm 0.12 \text{ d}$  [30], thus demonstrating that the escape of radioactive atoms during our measurement was negligible. Hence the

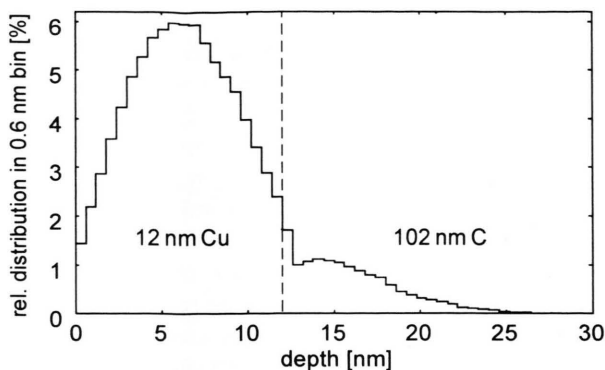


Fig. 1. The  $^{35}\text{S}$  concentration profile inside the source calculated with the program TRIM [28, 29].

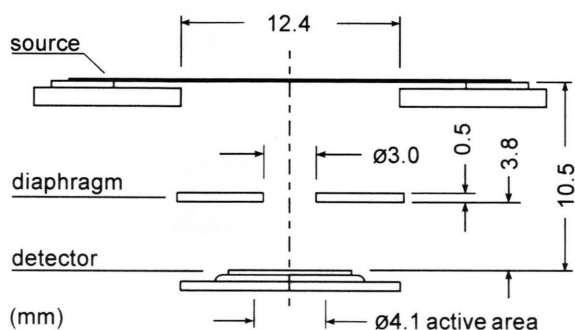


Fig. 2. Geometry of the experiment. Dimensions are given in mm.

response function, calculated with all  $\beta$  rays originating from the source, was based on a sound assumption.

## 2.2. Semiconductor Spectrometer

The set-up inside the vacuum chamber as shown in Fig. 2 consisted of the  $^{35}\text{S}$  source, a 0.5 mm thick copper diaphragm with a 3 mm hole, a silicon detector of the PIN-type and a preamplifier. The detector was a photodiode S 1722-1 from Hamamatsu with an active area of 4.1 mm in diameter, where the entrance window had been removed. According to the manufacturer, the diode had been made using a 200  $\mu\text{m}$  silicon wafer; the  $\text{SiO}_2$  dead layer amounts to 150 nm and the p layer to 20 nm whereas the active thickness exceeds 197  $\mu\text{m}$  when fully depleted (bias voltage  $U_D = -100$  V). This thickness was sufficient for our purpose (see Section 3.4). The detector volume of less than 3 mm<sup>3</sup> was well suited to keep the background low.

The detector was mounted via a brass plate directly to a brass housing for the Digitex HIC-1577 preamplifier, which is especially designed for the use with small silicon detectors. The housing was fixed on a block of copper with a Peltier device for cooling in between. This block led the heat of the Peltier device outside the vacuum chamber and was cooled with an aluminum bar blown at by a fan. The temperature was measured with a Pt100 resistor at the housing and was kept above 0 °C to avoid a frozen layer on the detector, and below 9 °C to lower the leakage current and thus the noise of detector and preamplifier. The preamplifier was supplied with  $\pm 12$  V from a stabilized power device. The wiring for the test input was removed during data taking. The vacuum was kept in the range of 0.4–1.1 Pa. The pulses of the preamplifier were fed through an amplifier Tenelec TC205A to a multichannel analyzer Canberra MCA 35+.

The whole electronic circuitry was tested with an accurate pulse generator and a high-accuracy attenuator. The linearity turned out to lie within +0.10 and –0.55% in the pulse height range used for the analysis. The resolving width of the system was measured using seven conversion-electron lines from 25 to 235 keV of active ThB deposit. The FWHM was found to be constant over the interesting area and equal to 3.3 keV. It is mainly due to the electronics.

## 2.3. Measurement

In the whole experiment, 34 spectra of the  $^{35}\text{S}$  decay with various exposure times from 4 to 86 h were taken in two runs (A, B) of about one month each, separated by four days. The leakage current of the detector was in the range 1 to 3 nA. The total exposure time using the  $^{35}\text{S}$  source was about 810 h with a dead time of 0.4% for the multichannel analyzer as the slowest device in the electronic chain; the dead time of the analyzer does not distort the spectral shape. Thus there was no need for a pile-up correction in the analysis. The spectra were recorded using the full resolution of the multichannel analyzer (8192 channels) but were rebinned to 1024 channels for the analysis, having a channel width of about 0.24 keV. At 150 keV, where the kink due to a possible 17 keV neutrino is expected, about 107 000 cts/keV were collected and at 180 keV about 200 cts/keV of background were measured.

Three tests with active ThC deposit were performed: before run A, before run B and thereafter. The

amplification of the system, determined using the conversion electron lines, varied within  $\pm 0.5\%$  over the whole time, indicating a drift in the electronic system over the two months. However there was no drift observed in the individual ThB spectra. Especially the second test over about 28 h showed the same line-width as observed in the remaining ThB spectra.

After the measurements with  $^{35}\text{S}$  and ThC the shape of the background was measured for 96 h.

### 3. Computer Simulations

#### 3.1. General Approach

Numerous flexible computer programs have been developed (e.g. [31, 32]) as part of the effort to understand the interaction of high energy charged and neutral particles with matter. In these programs, multiple-scattering theories and “condensed history” methods are employed to determine electron energy loss and scattering after completing a step of predetermined macroscopic length. This approach results in a considerable reduction of the required computer time but introduces additional approximations into the physical model of the electron slowing down process. For example, a shortcoming of the EGS4 computer code [32] concerning electron backscattering has been recently pointed out by Bielajew *et al.* [33]. Baró *et al.* [34] treated a simplified Monte Carlo simulation of elastic electron scattering in limited media.

In this work, we attempted the highest attainable accuracy of the theoretical model describing electron interaction with various parts of our experimental set-up regardless of increasing requirements of computer time. Our effort appears us to be justified by the necessity to treat even minor effects that might create or hide a heavy neutrino signature in the  $\beta$  spectrum.

#### 3.2. Physical Model

In our Monte Carlo calculations, we treat the electron interaction with matter as a random succession of independent single scattering events. We assume that the coherent scattering effects, such as channeling and diffraction, are negligible. The real electron trajectory is simulated as a zigzag path composed of undisturbed parts that are interrupted by sudden scattering processes.

In the elastic electron scattering by a target atom, only the electron direction is changed, whereas energy

loss and change in direction may occur in an inelastic collision with a single electron or electrons in collective excitation.

We utilize the relativistic electron-atom cross-sections  $d\sigma_{\text{el}}/d\Theta$  tabulated for various angles  $\Theta$  and electron energies by Riley *et al.* [35]. We notice that this tabulation is somewhat rough at the smallest scattering angles in the case of lower atomic numbers and higher electron energies. Thus it can happen that the function  $(d\sigma_{\text{el}}/d\Theta) \sin \Theta$  has its maximum within the interval of the first tabulation step, i.e. between 0 and  $0.5^\circ$ . Therefore, we derived four intermediate values of  $d\sigma_{\text{el}}/d\Theta$  in the following way. We suppose the functional dependence of the Rutherford screened formula

$$\frac{d\sigma_{\text{el}}}{d\Theta} \propto \frac{1}{(1 - \cos \Theta + \kappa)^2} \quad (1)$$

with  $\kappa$  as the screening parameter to be valid for  $0^\circ \leq \Theta \leq 0.5^\circ$ .  $\kappa$  was determined from the ratio of the  $d\sigma_{\text{el}}/d\Theta$  values [35] at  $0^\circ$  and  $0.5^\circ$  and applied to (1) to obtain  $d\sigma_{\text{el}}/d\Theta$  for 0.1; 0.2; 0.3 and  $0.4^\circ$ .

The total elastic cross section,

$$\sigma_{\text{el}} = 2\pi \int_0^\pi \frac{d\sigma_{\text{el}}}{d\Theta} \sin \Theta d\Theta, \quad (2)$$

gives the elastic mean free path

$$\lambda_{\text{el}} = \frac{1}{n \sigma_{\text{el}}}, \quad (3)$$

where  $n$  is the number of scattering atoms per unit volume.

The distribution of electron energy losses  $w$  was determined from the derivative of the inverse mean free path  $\lambda_{\text{in}}^{-1}$ , giving the differential inverse mean free path (DIMFP) for elastic interactions,  $\frac{d(1/\lambda_{\text{in}})}{dw}$ . This

quantity is usually available in the range from 0 to 100 eV (e.g. [36, 37]) and towards higher energy losses its shape has to be extrapolated using a reasonable model. We applied the  $1/w^2$  dependence proposed by Liljequist [38]. The necessary condition to obtain realistic results is

$$w_{\text{av}} = S \lambda_{\text{in}}, \quad (4)$$

where  $w_{\text{av}}$  and  $S$  are the mean energy loss and the stopping power, respectively.  $S$  and  $\lambda_{\text{in}}$  are available in the literature [39, 40], and the condition (4) can be satisfied by a proper choice of the point where the



DIMFP and  $1/w^2$  functions are joined together. The values of  $w_{\text{av}}$  are calculated from the formula

$$w_{\text{av}} = \frac{\int_{w_{\text{min}}}^{w_{\text{max}}} w \frac{d(1/\lambda_{\text{in}})}{dw} dw}{\int_{w_{\text{min}}}^{w_{\text{max}}} \frac{d(1/\lambda_{\text{in}})}{dw} dw}. \quad (5)$$

The angular deflection  $\Theta_{\text{in}}$  of the inelastically scattered electron was determined with the relation

$$\frac{d\sigma_{\text{in}}}{d\Theta_{\text{in}}} = c_E \frac{\Theta_E}{\Theta_{\text{in}}^2 + \Theta_E^2}, \quad (6)$$

where  $\Theta_E$  equals  $w/2E$  and  $E$  is the energy before the collision [41, 42]. The proportionality constant  $c_E$  is determined by the value of the total inelastic cross section for the energy  $E$ . Generally, the angular deflections  $\Theta_{\text{in}}$  are much smaller than the deflections in elastic scattering.

The steplength  $l$  between two successive collisions ( $l \in (0, \infty)$ ) is a random variable with the distribution  $f(l) = \lambda_{\text{tot}}^{-1} \exp(-l/\lambda_{\text{tot}})$ , where  $\lambda_{\text{tot}}$  is the total mean free path,

$$1/\lambda_{\text{tot}} = 1/\lambda_{\text{el}} + 1/\lambda_{\text{in}}. \quad (7)$$

$l$  is then determined by  $l = -\lambda_{\text{tot}} \ln(R)$ , where  $R \in (0, 1)$  is a uniformly distributed random number.

The accuracy of the results in the Monte Carlo simulation does not only depend on the physical model applied, but also on the quality of the available input data. In particular, the differential elastic cross-sections [35] are tabulated in relatively rough steps at higher energies and the inelastic mean free paths are scarcely known in the range of hundreds of keV.

The Monte Carlo calculations of this work were carried out on a Micro VAX 3100 computer using the uniform random number generator RNDM 2 with the period of about  $5 \times 10^{18}$  numbers, available from the CERN library.

### 3.3. Comparison with other Models

Our model and computer codes were tested in simple situations with known characteristics (see e.g. [43]). In order to have a closer look to the task similar to those of this work, we calculated the energy spectrum of 100 keV electrons that hit a flat surface of bulk silicon perpendicularly and are backscattered with an energy loss into the backward hemisphere. Our spectrum, displayed in Fig. 3, corresponds to  $5 \times 10^5$  incident electrons. We obtain a total backscattering coefficient  $\eta$  of 0.168. For comparison the results of two

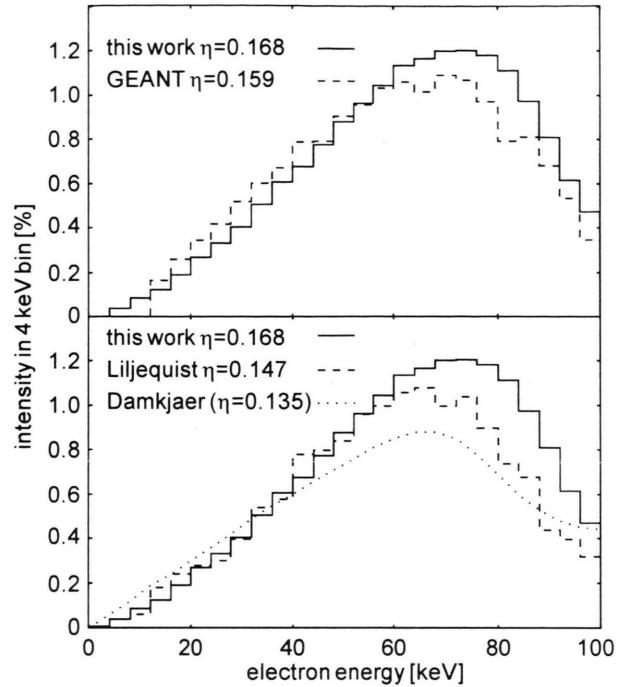


Fig. 3. Various simulations concerning perpendicular incidence of 100 keV electrons on bulk silicon (see text).

other simulations [31, 44] are also shown, together with the respective  $\eta$  values.

There is rather good agreement among the spectra of backscattered electrons calculated by various authors in the energy interval of backscattered electrons from 0 to about 50 keV. For higher energies, systematic deviations appear that show up also in different values of  $\eta$ . At the same time, there is a large scatter among experimental values of the backscattering coefficients of 100 keV electrons incident perpendicularly on bulk silicon. For example,  $\eta = 0.15$  and  $0.135$  were reported by Planskoy [45] and Damkjaer [46], respectively, and in more recent work  $\eta \approx 0.18$  (147 keV) by Arnoldi [47], performed in our laboratory at Garching, and  $\eta \approx 0.17$  (150 keV) by Chen *et al.* [20]. Arnoldi utilized the same silicon photodiode that was employed in this work. He irradiated it with electrons monochromized by a magnetic spectrometer [48].

For completeness, the analytical function suggested by Damkjaer [46] to describe the effect of electron backscattering in silicon detectors, normalized to his measured values of  $\eta$ , is exhibited in Fig. 3, too. We find no gap above zero energy loss, as reported in [13],

are, however, not sure to what extent this gap is in reality due to the diode dead layer.

The differences in the spectra of backscattered electrons as well as in the backscattering coefficients of various origin, as summarized in Fig. 3, demonstrate the present state-of-the-art for calculations and experiments of this type.

### 3.4. Calculations for the Experimental Set-up

The described Monte Carlo techniques were applied to obtain the response function of our experimental set-up. The main parts of the assembly used in this experiment were investigated separately to gain information about their individual influence. Electron energies  $E_0$  of 20; 50; 100 and 167 keV were used to examine the energy dependence. The mechanism of charge production and collection inside the detector was not simulated, thus the resolution of the system was taken from the experiment.

To investigate the effect of the geometry, calculations in three dimensions were performed, assuming a source of monoenergetic electrons without energy loss or angular deflection inside the source (ideal-source model). The angular distribution of electrons hitting the detector directly (direct electrons), as obtained by a simple Monte Carlo simulation, is shown in Figure 4. The electrons of interest are emitted with  $\cos \varepsilon > 0.8$ , where  $\varepsilon$  is the angle to the source normal.

The energy loss inside the source was calculated using the theoretical concentration profile (Figure 1). The length of the source determined by the source holder is 12.4 mm. The results are shown in Fig. 5(a). The distributions in relative energies  $E/E_0$  are nearly the same for 100 and 167 keV, whereas the energy

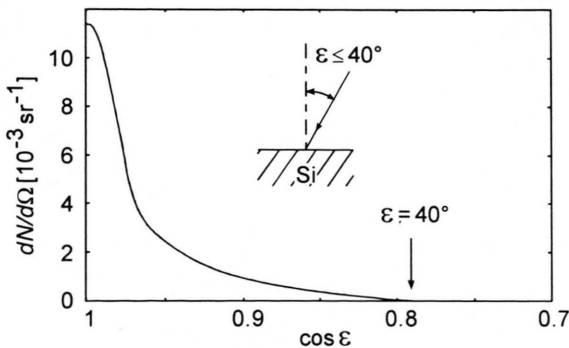


Fig. 4. Angular distribution of direct electrons hitting the detector.

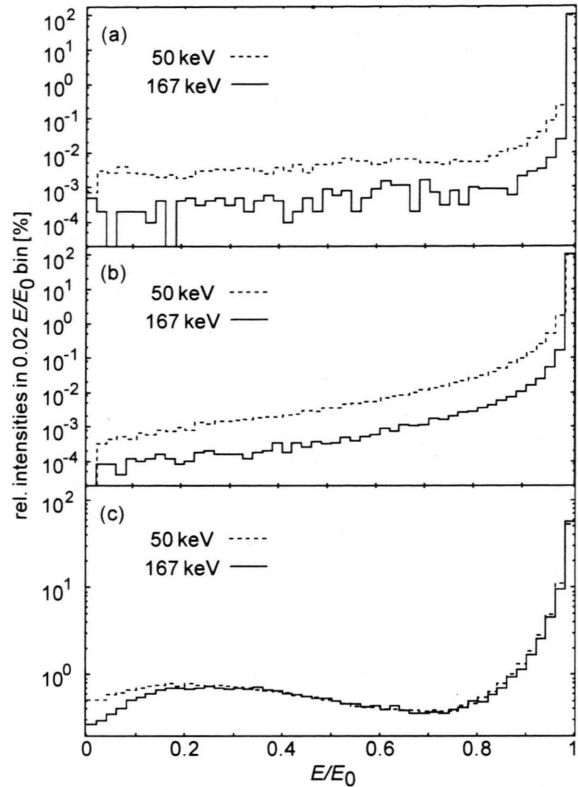


Fig. 5. Effects of various parts of the setup on originally monoenergetic electrons of  $E_0 = 50$  and 167 keV. (a) Energy distribution of electrons coming out of the source in a cone with  $\cos \varepsilon > 0.8$ . (b) Energy distribution of electrons emitted from an ideal source transmitted through dead layer of the detector. (c) Energy deposited inside the sensitive layer by indirect electrons coming from an ideal source.

dependence is not negligible for  $E \leq 70$  keV, as also denoted in [43]. The angular dependence of the energy distribution is small in the range of  $\cos \varepsilon > 0.8$  and was neglected.

The dead and p layers of the detector were approximated by a single layer of 170 nm silicon. Its influence on direct electrons was calculated assuming an ideal source and the angular distribution of direct electrons mentioned above; note that this differs from the assumptions in the case of Figure 3. The effect of the dead layer was found to be greater than that of the source (Fig. 5(b), Table 2).

The same ideal-source model was used in the calculation of backscattering by the sensitive layer of the detector. The shapes of the energy distributions of electrons backscattered in this experiment are slightly different from those of normal incidence. The coeffi-

cients of backscattering are listed in Table 2. For 167 keV electrons, 0.036% of the incident electrons penetrated through the sensitive layer which was assumed to be 190  $\mu\text{m}$  thick. This thickness is somewhat lower than the real value of 197  $\mu\text{m}$  (cf. Sect. 2.2) and is sufficient for the task.

Electrons hitting the detector after being scattered by the diaphragm (indirect electrons) were investigated in a slightly different way. Assuming an ideal source, the energy and angular distributions of indirect electrons were calculated taking into account the geometry of the set-up in three dimensions. The amount of indirect electrons scattered into the detector additionally to the direct ones is given in Table 2. The rather high values of about 10% are due to the shape of the source (cf. Section 2.1).

The angular distribution of the indirect electrons differs from that of the direct ones. The energy deposited inside the depleted volume of the detector (Fig. 5(c)) was calculated assuming the inner part of the diaphragm to be a radioactive source emitting electrons with the energy and angular distribution mentioned above.

#### 4. Data Analysis

##### 4.1. Theoretical Shape of the $\beta$ Spectrum

The energy distribution of the  $\beta$  particles from the decay with a massless neutrino,  $m_{\nu L} = 0$ , and a neutrino of mass  $m_{\nu H} = 17 \text{ keV}/c^2$  was expressed by

$$\frac{dN(E, |U_{eH}|^2)}{dE} \propto W p F(E) (E_{\max} - E)^2 \times \begin{cases} \left(1 + |U_{eH}|^2 \left( \sqrt{1 - \frac{m_{\nu H}^2 c^4}{(E_{\max} - E)^2}} - 1 \right) \right); & E < E_{\max} - m_{\nu H} c^2; \\ (1 - |U_{eH}|^2); & E_{\max} - m_{\nu H} c^2 < E < E_{\max}, \end{cases} \quad (8)$$

with  $W$  as the total energy of the electron,  $p$  the electron momentum and  $|U_{eH}|^2$  the branching ratio for heavy neutrinos;  $F(E)$  is the Fermi function, which was calculated by Ryšavý [50] in a 0.1 keV mesh.  $E_{\max}$  amounts to  $167.18 \pm 0.12 \text{ keV}$  [49].

The shape, given in (8), is to be folded with the response functions of the various parts of the experimental set-up. As described in Sect. 3.4, these functions were calculated by the Monte Carlo method for four energies  $E_0 = 20$  to 167 keV. To obtain the re-

sponse for an intermediate  $E_0$ , an interpolation [51] was used.

The theoretical shape in (8) was first folded with the source function. Direct and indirect electrons were handled in a different way (see Section 3.4). The corresponding response functions obtained by additional folding procedures are shown in Figure 6. The spectra for direct and indirect electrons were added with a proper weighting factor (Table 2). The result was convoluted with a Gaussian line of 3.3 keV FWHM giving the shape of the expected  $\beta$  spectrum  $dN^{\text{th}}(E, |U_{eH}|^2)/dE$ .

The shape of the background was determined using a measurement without radioactive source. The spectrum was well described by an empirical function  $b_0 B(i)$  with  $B(i) = \exp(b_1 i + b_2 i^2)$  in the interval from channel  $i = 300$  to  $i = 900$  (corresponding to about 75

Table 2. Fractions of absorbed or scattered electrons and mean energy losses for various parts of the assembly. Fractions are in % and energy losses in % of  $E_0$ .

	$E_0$ [keV]			
	20	50	100	167
Direct electrons				
$\langle \Delta E \rangle$ (source)	0.86	0.14	0.04	0.02
$\langle \Delta E \rangle$ (dead layer)	1.5	0.46	0.17	0.10
fraction absorbed (dead layer)	1.7	0.20	0.05	0.02
fraction $\eta$	18.5	18.1	17.9	17.5
Indirect electrons				
fraction of direct	8.7	9.3	9.7	10.0

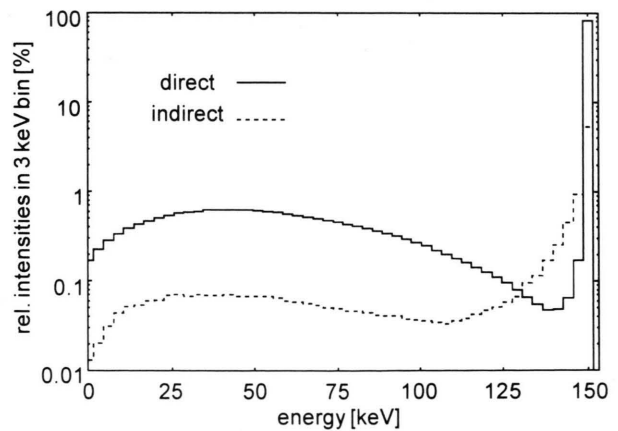


Fig. 6. Response functions for 150 keV electrons before convolution with Gaussian line for direct and indirect electrons. The normalization of the distributions corresponds to experiment.

to 220 keV) for the spectra rebinned to 1024 channels. The parameters  $b_1$  and  $b_2$  were determined to be  $-5.8(5) \times 10^{-3}$  per channel and  $2.7(5) \times 10^{-6}$  per channel squared, respectively; the amplitude  $b_0$ , expressed in counts per channel, is a free parameter in the following analysis.

A measured pulse height spectrum was then assumed to be described by

$$\langle N^{\text{exp}}(i) \rangle = a_0 \frac{dN^{\text{th}}(E(i), |U_{\text{eH}}|^2)}{dE} c_1 + b_0 B(i), \quad (9)$$

where  $a_0$  is the amplitude of the  $\beta$  spectrum in units of cts and  $E(i)$  the energy corresponding to the channel  $i$  given by  $E(i) = c_0 + c_1 i$ , where  $c_0$  is the offset energy in keV and  $c_1$  the constant channel width in keV/channel.

#### 4.2. Analysis of the Individual Spectra

The compatibility of the 34 individual spectra was tested by a model-independent method described in [52]. This test showed that there were small drifts during the two months measurement as indicated already by the ThB calibrations (see Section 2.3). Therefore the calibration constants  $c_0$  and  $c_1$  were determined from each individual spectrum itself, fitted along with  $a_0$  and  $b_0$  for a given mixing probability  $|U_{\text{eH}}|^2$  for each individual spectrum, using the method of maximum likelihood. In this way we were able to reproduce the measured shape within less than 1% down to 60 keV.

To obtain the mixing probability  $|U_{\text{eH}}|^2$  from the whole set of 34 spectra, the  $\chi^2$ -parabola with respect to  $|U_{\text{eH}}|^2$  was calculated by adding the  $\chi_j^2(|U_{\text{eH}}|^2)$  values ( $j=1, \dots, 34$ ) of the individual spectra. Each  $\chi_j^2(|U_{\text{eH}}|^2)$  was determined in the interval from about 125 to 210 keV with four free parameters using 401 channels. Thus we had 397 degrees of freedom for each individual spectrum and 13 498 for the whole set. This procedure is equivalent to fitting all  $4 \times 34 = 136$  parameters simultaneously, because the spectra were measured independently.

#### 4.3. Results

The admixture of a 17 keV neutrino was evaluated to be  $|U_{\text{eH}}|^2 = (-0.06 \pm 0.36)\%$  ( $1\sigma$  error) with a reduced  $\chi_r^2 = 0.992$ , giving an upper limit of 0.59% at 95% CL. The same procedure, neglecting the indirect electrons, gave  $|U_{\text{eH}}|^2 = (0.28 \pm 0.34)\%$ ,  $\chi_r^2 = 0.992$ ;

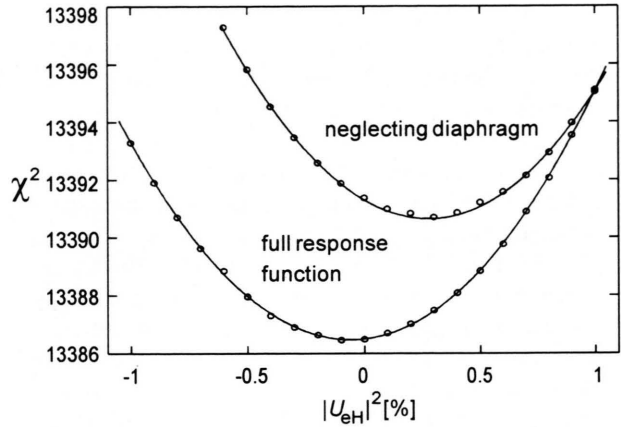


Fig. 7.  $\chi^2$ -parabolas with respect to mixing probability.

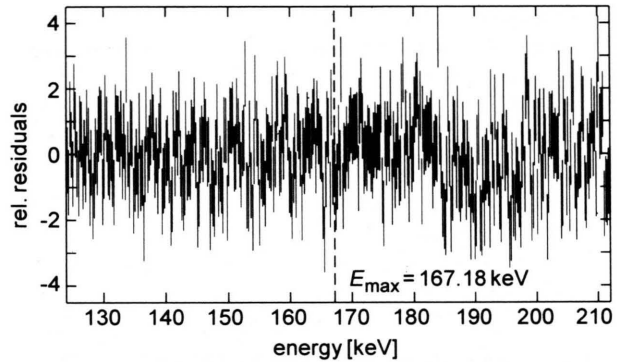


Fig. 8. Relative residuals of the combined spectra.

note that the errors in the two evaluations of the spectra are not independent but, on the contrary, strongly correlated. So the difference of  $0.28\% - (-0.06)\% = 0.34\%$  is statistically significant. This is corroborated by the corresponding  $\chi^2$ -parabolas as shown in Figure 7.

To obtain an impression of the residuals, the spectra were added according to their determined calibration in the case of  $|U_{\text{eH}}|^2 = 0$ . The sum was then described by (9) with the two amplitudes  $a_0$  and  $b_0$  as parameters. The relative residuals are shown in Figure 8.

## 5. Discussion

### 5.1. The $^{35}\text{S}$ Source Quality

Measurements of the  $^{35}\text{S}$   $\beta$  spectrum aiming to determine the neutrino rest mass started almost half a



century ago. Since then, numerous studies of the  $^{35}\text{S}$   $\beta$  spectrum were carried out, mainly to search for the 17 keV neutrino. The sources were prepared by various techniques of wet chemistry with their uncertainty about source thickness and homogeneity. Apalikov *et al.* [17] evaporated methionine ( $\text{C}_5\text{H}_{11}\text{NO}_2\text{S}$ ), labeled with  $^{35}\text{S}$ , on a conducting glass in vacuum, while Altitzoglou *et al.* [16] implanted 60 keV  $^{35}\text{S}^+$  ions into a carbon backing. Most recently, Bowler and Jelley [53] repeated the experiment of Hime and Jelley [5] and found that  $^{35}\text{S}$  sources, prepared by chemical adsorption of  $\text{Ba}^{35}\text{SO}_4$ , are clumped and locally thick, causing an energy loss of about 0.3 keV at 150 keV electron energy. The authors of [53] showed that neglect of this additional energy loss mimics presence of a 17 keV neutrino.

It is an advantage of our method that we know the composition, thickness and depth distribution of our  $^{35}\text{S}$  source; needless to say that source and backing are unusually thin.

### 5.2. Instrumental Response Function

One of the crucial points in the analysis of a measured  $\beta$  spectrum is the exact knowledge of the response of the whole set-up to monoenergetic electrons. Since radioactive decay is often accompanied by emission of internal-conversion or Auger electrons, one would expect that the instrumental response function can be measured with sufficient accuracy.

However, in the precise analysis of continuous  $\beta$  spectra one needs to know not only the exact shape of the full-energy peak of the detector response function but also the low-energy tail which extends with extremely small intensity up to zero kinetic energy (see e.g. Fig. 5); such a tail cannot be deduced from conversion line experiments with the accuracy needed for delicate shape measurements of continuous spectra. Our thorough parameter-free calculations of the response function for the whole instrumental set-up led to perfect agreement of calculated and measured  $\beta$  spectra for energies above 120 keV (cf. Section 4.3); the deviations were smaller than 1% down to 60 keV. Insufficient knowledge of the response function can lead to erroneous conclusions about a heavy-neutrino admixture as exemplified recently by numerical studies [54, 55]. Indeed, the most striking example is the recent experiment on the  $^{35}\text{S}$   $\beta$  spectrum taken with a Si(Li) spectrometer at Oxford. Hime and Jelley [5] employed the conversion electron lines of  $^{57}\text{Co}$  and

$^{109}\text{Cd}$  to derive the response function of their apparatus and supported these calibration measurements with some calculations of energy loss and backscattering within their detector. The authors found in their high-statistics spectra the 17 keV neutrino with a mixing probability of  $(0.84 \pm 0.06 \pm 0.05)\%$ .

Following Piilonen and Abashian [56], Hime [12] considered additional scattering effects in the reanalysis of the  $^{35}\text{S}$  data [5], especially electron scattering on the diaphragm between source and detector; note that this scattering is implicitly contained already in the experimental response function for conversion lines! The application of this more complex response function did not confirm the previous claim for the 17 keV neutrino, and an upper limit of its admixture was put to 0.35% at 90% CL [12].

In our experiment, the influence of indirect electrons scattered by the diaphragm to the detector proved to be even stronger due to the shape of our source. Neglecting this effect in the analysis creates a false 17 keV neutrino admixture of 0.3%.

In our Monte Carlo calculations based on individual scattering events, we do not meet the difficulties described by Hime [12] when dealing with thin layers, as e.g. the source backing or the detector dead layer. It should be mentioned that Monte Carlo calculations concerning electron scattering were necessary in recent experiments employing guiding magnetic fields, too [13, 15], and are indeed very important there.

### 5.3. Shape Correction Factors

Some of the previously  $^{35}\text{S}$   $\beta$  spectra did not exhibit a shape compatible with theory even at higher energies, and their investigators introduced various functions to correct for this imperfection. For example, Apalikov *et al.* [17] applied the function  $[1 + \alpha(E_0 - E)] \times [1 + \alpha'(E_0 - E)^2]$  with  $\alpha$  and  $\alpha'$  as additional fitting parameters. Although they reached a straight Kurie-type plot in this way, the above correction amounted to 14.6% of the measured counting rate when going from  $E = E_0 = 167$  keV to  $E = 120$  keV. In recent investigations, smaller, although not negligible, corrections were needed.

Bonvicini [57] claims to have shown by Monte Carlo simulations that a massive neutrino in a  $\beta$  spectrum could very well be masked by a spectral “shape correction factor”. In our work, we did not need any artificial correction to the measured  $^{35}\text{S}$  spectrum in the range from 120 to 200 keV.

## 6. Conclusion

We have measured the  $\beta$  spectrum of  $^{35}\text{S}$  and did not find any indication for an admixture of a 17 keV neutrino to the customary light neutrino. Our analysis was based on the theoretical response function of the whole experimental set-up calculated by the Monte Carlo method *without any adjustable parameter*. We used a thin source on a thin backing. We admitted only low counting rates in order to make sure that the experimental spectral shape was not distorted by electronic effects such as pile-up (or effects induced by an electronic pile-up rejector). Although our upper limit for the 17 keV neutrino cannot compete with the latest experiments (e.g. [22]) in statistical precision, it is not far from the limit of the reanalyzed Oxford experiment [5, 12], before reanalysis considered as the strongest argument for the existence of a 17 keV neutrino.

In our model of single scattering events we could reliably treat the electron energy losses and the scattering in thin layers as well as in bulk material. In

particular, we took properly into account the intermediate electron scattering by the spectrometer diaphragm and demonstrated that its neglect generates a false admixture of the 17 keV neutrino.

## Acknowledgement

We are obligated to D. Liljequist for calculating a check example of electron backscattering using his approach. Thanks are due to M. Ryšavý for detailed calculations of the relativistic Fermi function, M. Fišer for advice concerning sulphur chemistry and V. Hnatowicz for discussion on ion implantation. We acknowledge help of V. Havránek and J. Rak in application of the computer codes TRIM and GEANT. Ch. Sh. is obliged to Volkswagenstiftung for financial support, and O. D. is grateful to Deutsche Forschungsgemeinschaft for a senior fellowship. N. D., Ch. Sh. and O. D. appreciate the hospitality of the E18 staff during their stay in Garching. The work was supported in part by the Grant Agency of the Czech Republic under contract No. 202/93/1146.

- [1] Ch. Weinheimer, M. Przyrembel, H. Backe, H. Barth, J. Bonn, B. Degen, Th. Edling, H. Fischer, L. Fleischmann, J. U. Groß, R. Haid, A. Hermann, G. Kube, P. Leiderer, Th. Loeken, A. Molz, R. B. Moore, A. Osipowicz, E. W. Otten, A. Picard, M. Schrader, and M. Steininger, *Phys. Lett. B* **300**, 210 (1993).
- [2] F. Boehm and P. Vogel, *Physics of massive neutrinos*. 2nd. Edn. Cambridge: University Press 1992.
- [3] R. L. Mößbauer, *Nucl. Phys. A* **553**, 15c (1993).
- [4] J. J. Simpson, *Phys. Rev. Lett.* **54**, 1891 (1985).
- [5] A. Hime and N. A. Jelley, *Phys. Lett. B* **257**, 441 (1991).
- [6] B. Sur, E. B. Norman, K. T. Lesko, M. M. Hindi, R.-M. Larimer, P. N. Luke, W. L. Hansen, and E. E. Haller, *Phys. Rev. Lett.* **66**, 2444 (1991).
- [7] A. Hime and J. J. Simpson, *Phys. Rev. D* **39**, 1837 (1989).
- [8] T. Ohi, M. Nakajima, H. Tamura, T. Matsuzaki, T. Yamazaki, O. Hashimoto, and R. S. Hayano, *Phys. Lett.* **160 B**, 322 (1985).
- [9] V. M. Datar, C. V. K. Baba, S. K. Bhattacharjee, C. R. Bhuiya, and Amit Roy, *Nature, London* **318**, 547 (1985).
- [10] J. J. Simpson and A. Hime, *Phys. Rev. D* **39**, 1825 (1989).
- [11] A. Hime and N. A. Jelley, D. Phil. Thesis. Preprint OUNP-91-21. Oxford University 1991.
- [12] A. Hime, *Phys. Lett. B* **299**, 165 (1993).
- [13] H. Abele, G. Helm, U. Kania, C. Schmidt, J. Last, and D. Dubbers, *Phys. Lett. B* **316**, 26 (1993).
- [14] A. V. Derbin, A. I. Egorov, V. N. Muratova, L. A. Popenko, S. V. Bakhlanov, and A. V. Chernyi, *Pis'ma Zh. Eksp. Teor. Fiz.* **58**, 1 (1993).
- [15] J. L. Mortara, I. Ahmad, K. P. Coulter, S. J. Freedman, B. K. Fujikawa, J. P. Greene, J. P. Schiffer, W. H. Trzaska, and A. R. Zeuli, *Phys. Rev. Lett.* **70**, 394 (1993).
- [16] T. Altizoglou, F. Calaprice, M. Dewey, M. Lowry, L. Piilonen, J. Brorson, S. Hagen, and F. Loeser, *Phys. Rev. Lett.* **55**, 799 (1985).
- [17] A. M. Apalikov, S. D. Boris, A. I. Golutvin, L. P. Laptin, V. A. Lyubimov, N. F. Myasodov, V. V. Nagovitsin, E. G. Novikov, V. Z. Nozik, V. A. Soloshchenko, I. N. Tikhomirov, and E. F. Tretyakov, *Pis'ma Zh. Eksp. Teor. Fiz.* **42**, 233 (1985).
- [18] J. Markey and F. Boehm, *Phys. Rev. C* **32**, 2215 (1985).
- [19] D. W. Hetherington, R. L. Graham, M. A. Lone, J. S. Geiger, and G. E. Lee-Whiting, *Phys. Rev. C* **36**, 1504 (1987).
- [20] M. Chen, D. A. Imel, T. J. Radcliffe, H. Herinkson, and F. Boehm, *Phys. Rev. Lett.* **69**, 3151 (1992).
- [21] S. Schönert, K. Schreckenbach, S. Neumaier, and F. von Feilitzsch, *Nucl. Phys. B (Proc. Suppl.)* **28 A**, 176 (1992).
- [22] T. Ohshima, H. Sakamoto, T. Sato, J. Shirai, T. Tsukamoto, Y. Sugaya, K. Takahashi, T. Suzuki, C. Rosenfeld, S. Wilson, K. Ueno, Y. Yonezawa, H. Kawakami, S. Kato, S. Shibata, and K. Ukai, *Phys. Rev. D* **47**, 4840 (1993).
- [23] H. Kawakami, S. Kato, T. Ohshima, C. Rosenfeld, H. Sakamoto, T. Sato, S. Shibata, J. Shirai, Y. Sugaya, T. Suzuki, K. Takahashi, T. Tsukamoto, K. Ueno, and K. Ukai, *Phys. Lett. B* **287**, 45 (1992).
- [24] G. E. Berman, M. L. Pitt, F. P. Calaprice, and M. M. Lowry, *Phys. Rev. C* **48**, R1 (1993).
- [25] M. Bahran and G. R. Kalbfleisch, *Phys. Lett. B* **291**, 336 (1992) and erratum at *Phys. Lett. B* **294**, 479 (E) (1992).
- [26] G. R. Kalbfleisch and M. Bahran, *Phys. Lett. B* **303**, 355 (1993).
- [27] E. Hechtel, *Nucl. Instrum. Meth.* **139**, 79 (1976).

- [28] J. F. Ziegler, J. P. Biersack, and U. Littmark, The stopping and ranges of ions in solids, Pergamon, New York 1985.
- [29] J. P. Biersack and L. G. Haggmark, Nucl. Instrum. Meth. **174**, 257 (1980).
- [30] E. Browne, R. B. Firestone, and V. S. Shirley, Table of radioactive isotopes, John Wiley & Sons, New York 1986.
- [31] R. Brun, F. Bruyant, M. Maire, A. C. McPherson, and P. Zanarini, GEANT3. Report DD/EE/81-1. Geneva, CERN 1987.
- [32] W. R. Nelson, D. W. O. Rogers, and H. Hirayama, The EGS4 code system. Stanford linear accelerator report SLAC-265. Stanford 1985.
- [33] A. F. Bielajew, R. Wang, and S. Duane, Nucl. Instrum. Meth. **B 82**, 503 (1993).
- [34] J. Baró, J. Sempau, J. M. Fernández-Varea, and F. Salvat, Nucl. Instrum. Meth. **B 84**, 465 (1994).
- [35] M. E. Riley, C. J. MacCallum, and F. Biggs, Atom. Data Nucl. Data Tables **15**, 443 (1975).
- [36] J. C. Ashley, J. J. Cowan, R. H. Ritchie, V. E. Anderson, and J. Hoelzl, Thin solid films **60**, 361 (1979).
- [37] H. Raether, Excitation of plasmons and interband transitions by electrons. Springer, Berlin, Heidelberg, New York 1980.
- [38] D. Liljequist, J. Phys. D: Appl. Phys. **11**, 839 (1978).
- [39] F. Salvat, J. D. Martinez, R. Mayol, and J. Parellada, J. Phys. D: Appl. Phys. **18**, 299 (1985).
- [40] S. Tanuma, C. J. Powell, and D. R. Penn, Surf. Interface Anal. **11**, 577 (1988).
- [41] J. Daniels, C. v. Festenberg, H. Raether, and K. Zeppenfeld, Springer tracts in modern physics (G. Hohler, ed.) **54**, 78 (1970).
- [42] R. Shimizu and Ze-Jung Ding, Rep. Prog. Phys. **55**, 487 (1992).
- [43] A. Špalek and O. Dragoun, J. Phys.G: Nucl. Part. Phys. **19**, 2071 (1993).
- [44] D. Liljequist, J. Appl. Phys. **57**, 657 (1985) and private communication 1994.
- [45] B. Planskoy, Nucl. Instrum. Meth. **64**, 189 (1968).
- [46] A. Damkjaer, Nucl. Instrum. Meth. **200**, 377 (1982).
- [47] T. Arnoldi, Diplomarbeit. Physik Department der Technischen Universität München 1991.
- [48] H. Daniel, P. Jahn, M. Kuntze, and B. Martin, Nucl. Instrum. Meth. **82**, 29 (1970).
- [49] G. Audi and A. H. Wapstra, Nucl. Phys. A **565**, 1 (1993).
- [50] V. Brabec and M. Ryšavý, Europhys. Lett. **21**, 811 (1993).
- [51] H. Akima, J. Assc. Comp. Mach. **17**, 589 (1970).
- [52] O. Dragoun, V. Brabec, V. Feifrlík, A. Kuklik, and F. Duda, Nucl. Instrum. Meth. **116**, 459 (1974).
- [53] M. G. Bowler and N. A. Jelley, Preprint OUNP-94-04. Oxford University 1994.
- [54] D. B. Cline and W. Hong, Mod. Phys. Lett. A **7**, 1201 (1992).
- [55] J. G. Hykawy, R. C. Barber, and K. S. Sharma, Nucl. Instrum. Meth. A **335**, 497 (1993).
- [56] L. Piilonen and A. Abashian, Progress in atomic physics, neutrinos and gravitation (G. Chardin, O. Fackler, and J. Trân Thanh Vân, eds.), p. 225. Gif-sur-Yvette, France: Editions Frontières 1992.
- [57] G. Bonvicini, Z. Phys. A **345**, 97 (1993).